RSC Advances

RSC Publishing

PAPER

View Article Online
View Journal | View Issue

Cite this: *RSC Advances*, 2013, **3**, 19104

Spontaneous formation of a large area, aligned, ordered, π-conjugated film with polarized fluorescence and an amplified spontaneous emission based on a liquid crystalline bi-1,3,4-oxadiazole derivative†

Songnan Qu,[a] Hongyu Zhang,[b] Yuejia Ma,[a] Junsheng Cao,[a] Shaohang Wu[a] and Xingyuan Liu*[a]

Received 20th March 2013,
Accepted 5th August 2013

DOI: 10.1039/c3ra41371c

www.rsc.org/advances

A large area, aligned, ordered, π-conjugated film of a liquid crystalline bi-1,3,4-oxadiazole derivative (BOXD-5) (up to several square millimeters) with polarized fluorescence ($I_{\max}/I_{\min}$ of 6.0, $\Phi_F = 72\%$) and a deep blue amplified spontaneous emission (ASE) ($\lambda = 405$ nm, threshold of about 2 kW cm^{-2}) can be easily obtained upon cooling from its nematic phase with homeotropic texture in air at room temperature without the help of an alignment layer. The laser damaged aligned BOXD-5 film sandwiched between untreated glass slides can ''self heal'' through an easy heating–cooling thermal process. Neither the polarized fluorescence nor the ASE phenomenon were observed in the vacuum evaporated film. The directional π–π interactions between the 1,3,4-oxadiazole rings and phenyl rings, and its peculiar mesophase sequence cooperatively sustain a large area, aligned, ordered, π-conjugated film with polarized fluorescence and an ASE.

Introduction

π-Conjugated molecules self-assembled to form functional π-conjugated supramolecular architectures have attracted great attention for organic electronic devices.[1] The strong π–π intermolecular interactions present in aggregated arrays of π-conjugated molecules are of benefit for charge transport and energy migration.[2] Many molecular designs have been proposed by expanding the π-conjugated segments to enhance the one directional face-to-face π–π intermolecular interactions. However, organic molecules with large π-conjugated segments rarely exhibit deep blue emissions and usually form *H*-aggregates which cause notorious fluorescence quenching.[3] It is a prime target to achieve both a high fluorescence efficiency and a continuous ordered, π-conjugated structure in one supramolecular system for efficient electroluminescent organic devices.[4,5]

Film morphology is a key factor in the performance of organic devices. Well aligned, ordered, π-conjugated films which contain molecules with the same orientation and transition dipole, can achieve polarized emissions, increased carrier mobility, decreased optical losses, and a low threshold ASE. These properties are attractive in materials science and organic electronics, and particularly for the electrically pumped organic laser.[6] Previously reported well aligned, ordered, π-conjugated films are usually based on external physical influences, such as aligned rubbed layers of polyimide (PI), which introduce considerable technological problems and do not benefit the carrier efficient injection, and subsequently lead to poor device performance. Large area, aligned π-conjugated films based on organic polymers can be relatively easily prepared with external physical influences. Polarized fluorescence, high carrier mobility, ASE and lasers have been reported in single crystals or nano/micro-wires based on small organic molecules.[7] However, it is still a challenge to prepare large area, well aligned, ordered, π-conjugated films based on small organic molecules even with external physical influences. Liquid-crystalline (LC) materials, which present a self-organizing ability, fluidity, and defect-free orientations with special treatment, have recently been recognized as having great advantages in the manipulation of optimized, high-efficiency organic electro-optic devices.[8] Preparing aligned films with attractive optical and electronic properties based on LC materials is a hot topic.

Lasers from solid state π-conjugated materials are one of the most attractive scientific achievements in the last two

---

[a] *State Key Laboratory of Luminescence and Applications, Changchun Institute of Optics, Fine Mechanics and Physics, Chinese Academy of Sciences, Changchun 130033, P. R. China. E-mail: liuxy@ciomp.ac.cn; qusn@ciomp.ac.cn*

[b] *Key Laboratory for Supramolecular Structure and Materials of Ministry of Education, College of Chemistry, Jilin University, Changchun 130012, P. R. China*

† Electronic supplementary information (ESI) available: Polarized PL spectra and POM images of the BOXD-5 large area, aligned, ordered, π-conjugated film and the vacuum evaporated film, and the calculated ground to excited state transition electric dipole moments (Au) of BOXD-5. See DOI: 10.1039/c3ra41371c

decades. However, there are considerable obstacles in laser action investigations and applications on organic materials due to their relatively low laser damage thresholds. The organic crystals or films can be damaged and can not be reused upon high energy laser pumping. It is strongly desirable to impart a ''self-healing'' capability to organic laser materials which would increase the useful lifetimes of these materials.[9]

We have previously successfully synthesized highly fluorescent liquid crystalline bi-1,3,4-oxadiazole derivatives.[10] An aligned crystalline microbelts film of BOXD-T3 with strong fluorescent emissions, a self-wave guided structure and an ultralow-threshold ASE (about 40 W cm^{-2}) was prepared in a solution processed method, while no ASE phenomenon was observed in the corresponding vacuum evaporated film.[11] There were some shortcomings in the solution processed method in our previous work: (1) the solvent might dissolve or affect the substrate organic layer; (2) the preparation was time-consuming (one day or longer); and (3) the laser pumping damaged film could not heal. There is a continuing interest in our group to explore the excellent performances of highly fluorescent bi-1,3,4-oxadiazole derivatives in solid-state optoelectronic applications. Herein, we report the spontaneous formation of a large area, aligned, ordered, π-conjugated film with highly polarized fluorescence and a deep blue ASE based on a linear shaped bi-1,3,4-oxadiazole derivative (BOXD-5). It was exciting to find that the laser damaged BOXD-5 film sandwiched between untreated glass slides could ''self heal'' through an easy heating–cooling thermal process. To the best of our knowledge, this is the first case of small organic molecules spontaneously self-assembling to form a large area, aligned, ordered, π-conjugated film without the help of an alignment layer, which possesses great advantages in the manipulation of optimized high-efficiency organic electronic devices.

Experimental section

Photoluminescence (PL) spectra were collected using a Hitachi F-4500 spectrometer and UV-visible absorption spectra were recorded on a Shimazu UV-3101PC spectrophotometer. Photoluminescence quantum yields were obtained in a calibrated integrating sphere (excitation wavelength: 330 nm) in a FLS920 spectrometer. The prepared BOXD-5 (Scheme 1) film was sandwiched between untreated glass slides (1.8 × 1.8 cm^2) and was placed in a calibrated integrating sphere for measurements. Fluorescence lifetimes were measured using a FLS920 time-corrected single photon counting (TCSPC) system. The optical and polarized optical microscopy (POM) and fluorescence microscopy images were recorded using an Olympus BX51TRF microscope. The light source for the fluorescence microscopy observation was a mercury lamp with a fluorescent filter cube, which provided excitation in the range of 330–385 nm, and collected emissions with wavelengths longer than 420 nm. The intensity of the fluorescence emission was measured using a built-in CCD camera along with the associated software. The emission spectra were recorded using an Ocean Optics Maya2000 Pro Fiber Optic Spectrometer. X-ray diffraction (XRD) was carried out using a Bruker Advance D8 X-ray diffractometer. ASE investigations were performed using a Nd:YAG laser (355 nm) with a repetition rate of 1 Hz and a pulse duration of about 10 ns. The laser power was detected by a Newport 2936C laser power meter. Film thicknesses were measured with a Filmetrics F20.

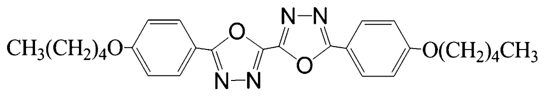

Scheme 1 Molecular structure of BOXD-5.

Results and discussion

Preparation of aligned films

BOXD-*n* (*n* = 5–16) mesophase behaviors were reported in our previous work.[10a] BOXD-5 exhibited a nematic phase, ordered smectic phase and crystal phase sequence during cooling from the isotropic phase (Fig. S1, ESI†). On slowly cooling BOXD-5 sandwiched between untreated glass slides from the isotropic state, birefringent droplets appeared, which subsequently vanished to give rise to a nematic phase with a large area of homeotropic texture (up to several square millimeters). There was no flow effect in this process. It was interesting to find that in air at room temperature a large area, aligned BOXD-5 film (up to several square millimeters) could be easily obtained upon quick cooling from the nematic phase with a homeotropic texture (Fig. 1a), which could ''self heal'' in a heating–cooling thermal process. No abrupt changes in brightness indicated the absence of domain boundaries in the film. The optical anisotropy indicated molecular alignment, since uniform darkness was observed when the molecular axis was perpendicular or parallel to the crossed-polarizers, as shown in Fig. 1(b), (d) and (f). The orientation of the film was stochastic during the heating–cooling thermal process, as shown in Fig. 1(g) and (h), which indicated that the alignment of the film was not caused by any aligning surface on the glass substrates. The thickness of the film was measured with a Filmetrics F20 and was found to be in the range of 7 to 8 μm. In addition, a large area, aligned BOXD-5 film that was not covered by glass was also prepared by moving the covered glass off along the same direction in the homeotropic nematic phase and then quickly cooling in air at room temperature, which may provide benefits for fabrication of organic electronic devices (Fig. S3, ESI†). The spontaneous formation of a large area, aligned film has not been observed in other liquid crystalline BOXD-*n* molecules, which might be because of the phase sequence (isotropic phase–nematic phase–ordered smectic phase–crystal phase) observed during cooling in BOXD-5.

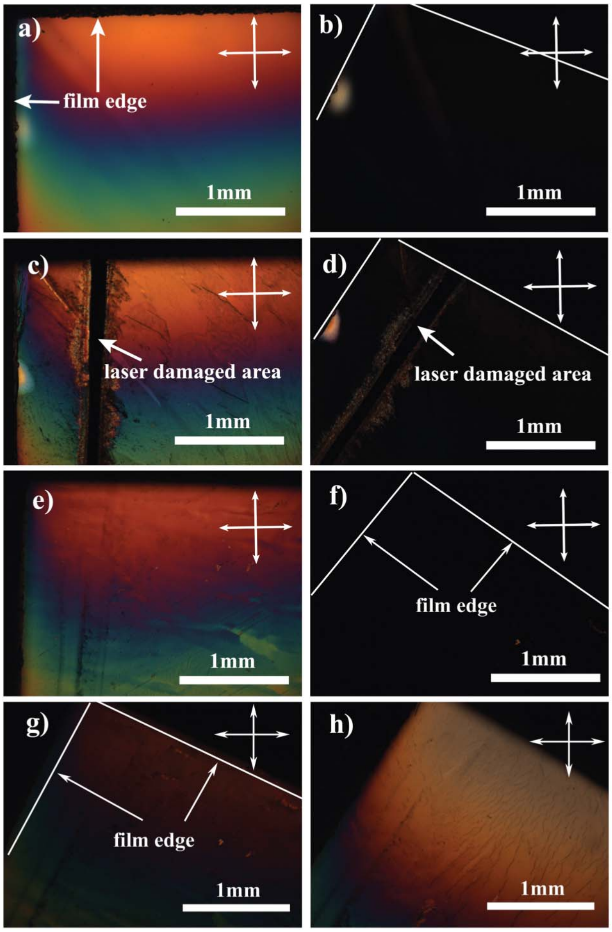

Fig. 1 POM images of the large area, aligned BOXD-5 film (a) sandwiched between untreated glass slides, (b) before laser pumping, (c) and (d) after high energy pumping (140 kW cm^{-2}), (e), (f) and (g) self healed by the heating–cooling thermal method at different rotating angles, and (h) during further heating–cooling thermal processes (white crossed arrows illustrate the crossed-polarizers).

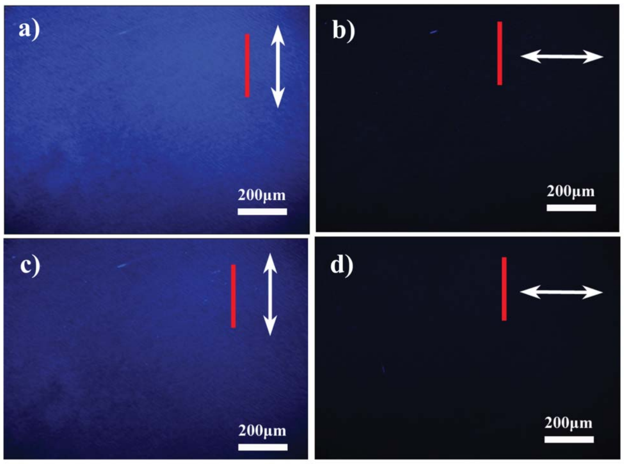

Fig. 2 (a) and (b) are polarized photoluminescence microscopy images, and (c) and (d) are polarized excited photoluminescence microscopy images of the aligned BOXD-5 film sandwiched between untreated glass slides (white arrows illustrate the directions of the polarizer and red arrows illustrate the BOXD-5 molecular orientations).

Optical properties

The aligned BOXD-5 film showed highly polarized fluorescence (λ_{max} = 391 nm, 403 nm, τ_F = 1.4 ns, Φ_F = 72%) with a maximal/minimal intensity ratio (I_{max}/I_{min}) of 6.0 (Fig. 2(a) and (b) and Fig. S4a, ESI†). From computations, the main transition dipole moment of BOXD-5 is parallel to the long molecular axis (Table S1, ESI†). Thus, the polarized fluorescence could help identify the molecular orientation in the film, since the maximum intensity is observed when the polarizer is parallel to the molecular orientation. Under polarized UV excitation, the most intense emission was obtained when the polarization of the incident UV light was parallel to the molecular orientation of the film, while the emission intensity diminished to a minimum when the polarization of the incident UV light changed by 90° from this position (Fig. 2(c) and (d)). The I_{max}/I_{min} detected in Fig. S4b, ESI† was about 4.5, indicating the absorption of this film was anisotropic. All of these observations indicated that the BOXD-5 molecules were regularly uniaxially oriented in this film. We also fabricated the vacuum evaporated BOXD-5 film (about 600 nm thick) for comparison. The vacuum evaporated BOXD-5 film also exhibited a high fluorescence efficiency (λ_{max} = 387, 402 nm, τ_F = 1.5 ns, Φ_F = 79%). Neither a uniform birefringence color change in POM, nor an anisotropic emission or absorption were observed in this film (Fig. S5, ESI†), indicating random molecular orientations. The photophysical properties of BOXD-5 in different states are listed in Table 1. It should be noted that the aligned BOXD-5 film exhibited a narrowed, blue shifted absorption band and an increased Stokes shift compared to the vacuum evaporated film (Fig. 3).

ASE properties and "self healing" behavior

A deep blue ASE (λ = 405 nm) was observed in the aligned BOXD-5 film, with a low threshold of about 2 kW cm^{-2} under a focused pumping laser source (355 nm) with the polarization of the pumping source parallel to the molecular orientation and perpendicular to the focused pumping stripe. No ASE phenomenon was observed when the polarization of the pumping source was perpendicular to the molecular orientation. When the excitation power was increased above the threshold, the intensity and the full width at half maximum (FWHM) of the ASE spectra were greatly increased and further narrowed, respectively (Fig. 4). At an excitation power of 35 kW

Table 1 Photophysical properties of BOXD-5 in different states at room temperature

	λ_{abs} (nm)	λ_{em} (nm)	Φ_F	τ_F (ns)	χ^2 [d]
CHL[a]	316	389	0.58	1.1	0.94
TA[b]	292	391, 403	0.72	1.4	0.91
VE[c]	309	387, 402	0.79	1.5	0.89

[a] CHL: chloroform solution (1 × 10^{-5} mol L^{-1}). [b] TA: thermal aligned, ordered film. [c] VE: vacuum evaporated film. [d] χ^2: fitting parameter.

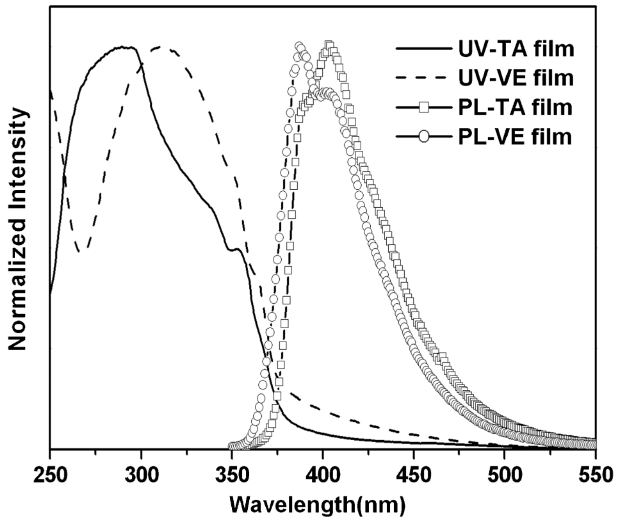

Fig. 3 UV-vis and fluorescence emission spectra of the aligned BOXD-5 film (TA) and the vacuum evaporated film (VE) (excitation wavelength: 330 nm).

cm^{-2}, the FWHM of the ASE spectrum was 4.5 nm. Further increasing the pumping energy damaged the film. Heating the laser damaged film sandwiched between untreated glass slides to its isotropic state caused the BOXD-5 liquid to flow slightly and the laser damaged area could easily fuse. During the cooling process, the laser damaged film sandwiched between untreated glass slides could "self heal" (Fig. 1(e)–(g), Fig. S2, ESI†), which provides distinct advantages in applications. The thickness of the "self-healed" film is nearly unchanged when measured with a Filmetrics F20. The laser damaged BOXD-5 film that was not covered by glass could not heal, but instead formed separate non-oriented aggregated islands after the thermal process. In contrast, no ASE phenomenon was observed in the vacuum evaporated film, although this film also exhibited a high fluorescence efficiency (Φ_F = 79%). The linear shaped BOXD-5 molecule exhibits an anisotropic absorption of excited light and a polarized emission. BOXD-5 molecules with random orientations can not efficiently absorb the polarized pumping laser and exhibit non-polarized emissions, which are not beneficial for photon correlated coupling for the amplification of light emissions. It can be concluded that the highly oriented packing of BOXD-5 with a polarized fluorescence plays an important role in realizing the ASE. All these factors contribute to the ASE phenomenon in the aligned BOXD-5 film.

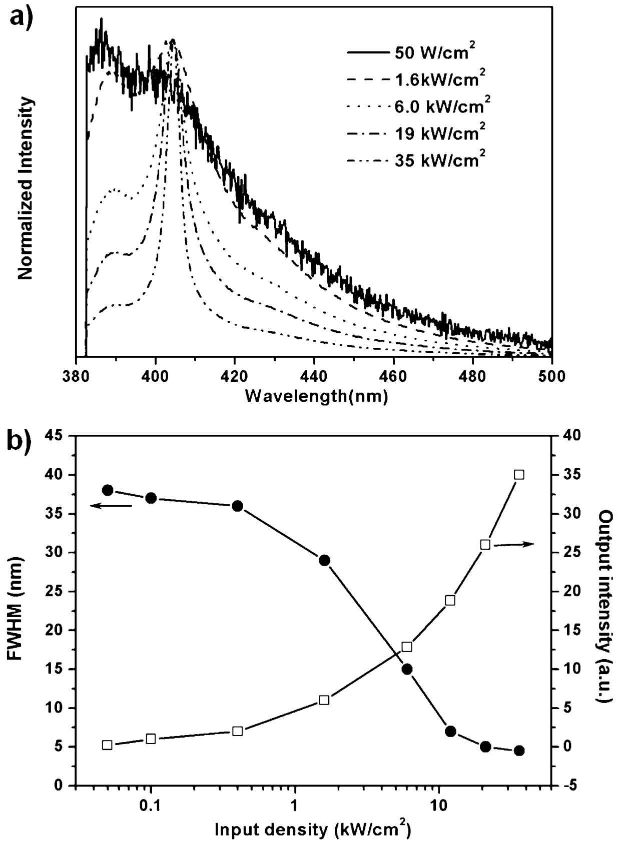

Fig. 4 (a) Normalized emission spectra of the aligned BOXD-5 film sandwiched between untreated glass slides under various optically pumped pulse densities. (b) The dependence of the output peak intensity (•) and the FWHM value (☐) of this film on the pumping density.

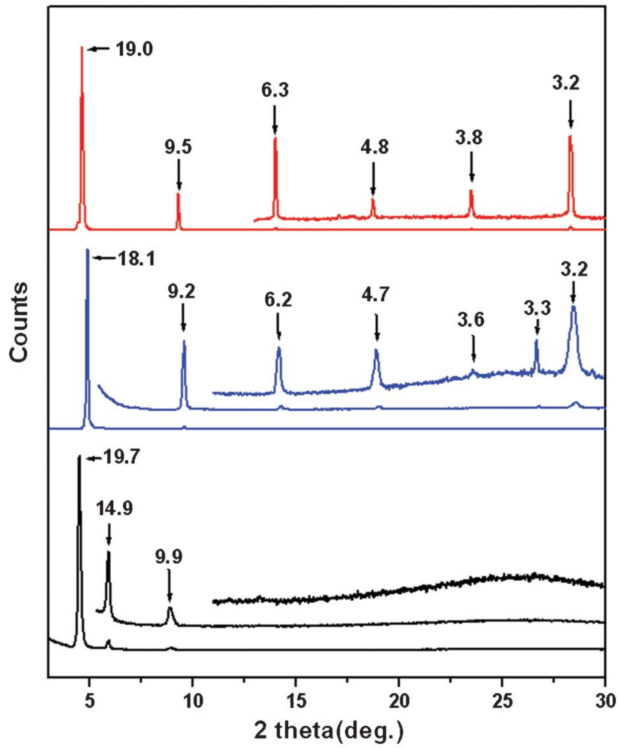

Fig. 5 XRD patterns of the BOXD-5 SmX phase at 170 °C (red lines), the aligned film (blue lines) and the vacuum evaporated film (black lines) at room temperature.

X-ray diffraction (XRD) investigations

The XRD pattern of the aligned BOXD-5 film shows a sharp, strong diffraction (18.1 Å) and up to fifth order diffractions, indicating its well-defined layered structure with sharp interfaces (Fig. 5). This is similar to its high temperature ordered smectic phase. Two diffractions (3.3 Å, 3.2 Å) and a halo centered around 26° were observed in the high-angle range. The layer space of the aligned BOXD-5 film was much shorter than the geometry optimized BOXD-5 molecular length with fully extended alkyl tails (30 Å). This indicated that the BOXD-5 molecules were highly tilted in the layers (about 36°). The XRD pattern of the vacuum evaporated BOXD-5 film shows a sharp strong diffraction (19.7 Å) and up to second order diffractions and an additional diffraction (14.9 Å) in the low-angle range, as well as a halo centered around 26° in the high-angle range, which indicated positional disorder. It can be concluded that the aligned BOXD-5 film and the vacuum evaporated BOXD-5 film exhibited smectic liquid crystal phases. The layer space of the aligned BOXD-5 film (18.1 Å) is shorter than that of the vacuum evaporated film (19.7 Å), indicating more slipped packing in the layers. The diffraction peak at 3.2 Å observed in the aligned BOXD-5 film and its SmX phase might be attributed to the distance between the BOXD-5 molecules in the layers. It can be concluded that the aligned BOXD-5 film exhibited a more ordered structure than the vacuum evaporated BOXD-5 film, which is beneficial for achieving organic electro-optic devices with good performances.

Theoretical calculations

The geometry of BOXD-5 in the ground state was calculated with the Becke3–Lee–Yang–Parr functional (B3LYP) methods. In the ground state, the four rings of the BOXD-5 molecule are coplanar, and the bond lengths of phenyl–oxadiazole and oxadiazole–oxadiazole are 1.45 Å and 1.44 Å respectively. These correspond well to the expected range for a C(sp2)–C(sp2) single bond (1.48 Å),[12] indicating that the rigid backbone of BOXD-5 is conjugated, which is beneficial for aggregating through intermolecular π–π interactions. The BOXD-5 dimer potential energy surface (PES) was computed as a function of the separate molecular plane (*d*), and the molecular shifts along the molecular long axis (*x*-displacement, or *x* for short) and the short axis (*y*-displacement, or *y* for short), as indicated in Fig. 6. The ground state PES was calculated with the M062x approach, which has a greatly improved performance for noncovalent interactions.[13] The ground state PES for $d = 3.2$ Å of the BOXD-5 dimer is shown in Fig. 6(b). It can be seen that the face-to-face molecular packing geometry has the highest energy due to unfavored electrostatic interactions. The two lowest minima predicted are M1: $x = 3.8$, $y = 0.8$ Å and M2: $x = 6.2$, $y = 1.2$ Å, with the binding energies calculated as $E_{\text{bin}} = 62.85$ kJ mol^{-1} and 59.10 kJ mol^{-1}, respectively (Fig. 6(c)). The BOXD-5 molecules are slipped, with an angle between the molecular plane and the aggregation direction of about 40° and 27° in M1 and M2, respectively. The angle between the molecular plane and the aggregation direction is decided between the presence of an *H*- or *J*-aggregate: above a theoretical value of 54.7° an *H*-aggregate is usually found, whereas in *J*-aggregates the molecules slip more with respect to each other, leading to a smaller angle.[14] The angles calculated in M1 and M2 are well below this theoretical value, indicating *J*-aggregates. It should be noted that the bi-1,3,4-oxadiazole rings are close to neighboring phenyl rings in both the M1 and M2 structures. It can be concluded that strong directional π–π intermolecular interactions between the 1,3,4-oxadiazole rings and phenyl rings are the driving force for making the BOXD-5 molecules highly tilted aggregates (*J*-aggregates), which agrees with the UV and XRD investigations of the aligned film and contribute to its fluorescence property in the solid state. Based on these results, it can be concluded that the directional π–π interactions between the 1,3,4-oxadiazole rings and phenyl rings and its peculiar mesophase sequence cooperatively sustain the aligned, ordered, π-conjugated film with polarized fluorescence and an ASE. Applications of the BOXD-5 aligned film in organic electro-optic devices are in process.

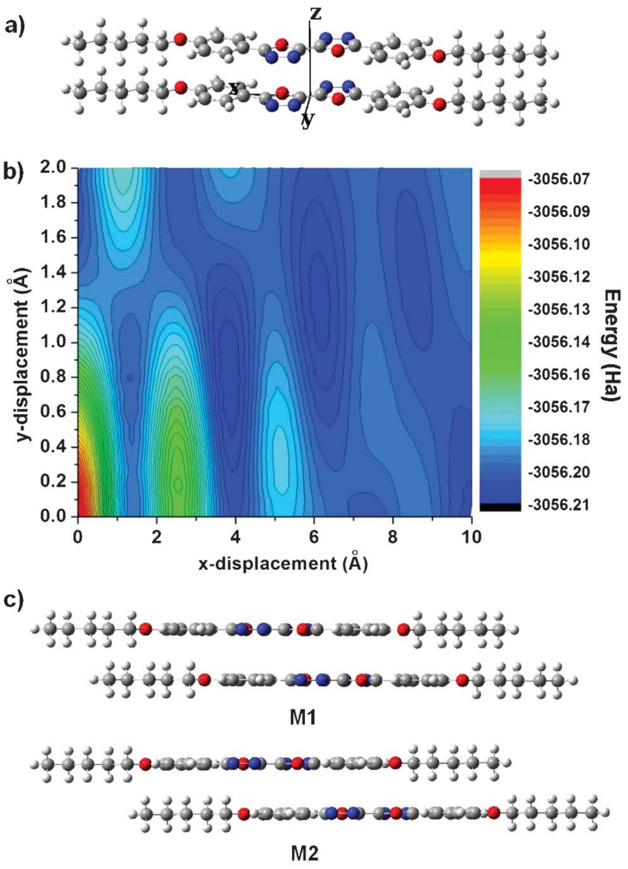

Fig. 6 (a) Intermolecular coordinates used for scanning the dimmer potential energy surface; (b) computed potential energy surface of dimmer BOXD-5 at the ground state; (c) calculated dimmer with the two lowest minima (M1 and M2).

Conclusions

In conclusion, a large area, aligned, ordered, π-conjugated film of BOXD-5 (up to several square millimeters) with polarized fluorescence ($I_{\text{max}}/I_{\text{min}}$ of 6.0, $\Phi_{\text{F}} = 72\%$) and a deep blue ASE ($\lambda = 405$ nm, threshold of about 2 kW cm^{-2}) can be easily obtained upon cooling from its nematic phase with homeotropic texture in air at room temperature without the help of an alignment layer. The laser damaged aligned BOXD-5 film sandwiched between untreated glass slides could "self heal" through an easy heating–cooling thermal process. Neither the polarized fluorescence nor the ASE phenomenon was observed in the vacuum evaporated film. The directional π–π interactions between the 1,3,4-oxadiazole rings and phenyl rings and its peculiar mesophase sequence cooperatively sustain the aligned, ordered, π-conjugated film with polarized fluorescence and an ASE. The interesting optical properties of the easily prepared, large area, aligned, ordered, π-conjugated film of a liquid crystalline bi-1,3,4-oxadiazole derivative could cause broad interest for further investigations and it might find useful applications in organic electronic devices.

Acknowledgements

We thank Prof. Min Li in Jilin University for her guidance in the synthesis of bi-1,3,4-oxadiazole derivatives. This work was supported by the CAS Innovation Program and National Science Foundation of China No. 51103144, 61106057, 61274126, 61007023 and Jilin Province Science and Technology Research Project No. 201101080.

References

1 (*a*) C. Joachim, J. K. Gimzewski and A. Aviram, *Nature*, 2000, **408**, 541; (*b*) J. L. Brédas, D. Beljonne, V. Coropceanu and J. Corni, *Chem. Rev.*, 2004, **104**, 4971; (*c*) S. R. Forrest, *Nature*, 2004, **428**, 911; (*d*) F. J. M. Hoeben, P. Jonkheijm, E. W. Meijer and A. P. H. J. Schenning, *Chem. Rev.*, 2005, **105**, 1491; (*e*) S. C. Lo and P. L. Burn, *Chem. Rev.*, 2007, **107**, 1097; (*f*) L. Zang, Y. Che and J. S. Moore, *Acc. Chem. Res.*, 2008, **41**, 1596; (*g*) L. C. Palmer and S. I. Stupp, *Acc. Chem. Res.*, 2008, **41**, 1674.

2 D. T. McQuade, J. Kim and T. M. Swager, *J. Am. Chem. Soc.*, 2000, **122**, 5885.

3 J. B. Birks, *In photophysics of Aromatic Molecules*, Wiley, London, 1970.

4 (*a*) K. Müllen and U. Scherf, *Organic Light-Emitting Devices: Synthesis Properties and Applications*, Wiely-VCH, Weinheim, Germany, 2006; (*b*) H. Yersin, *Highly Efficient OLEDs with PhosphorescentMaterials*, Wiely-VCH, Weinheim, Germany, 2008.

5 (*a*) M. Muccini, *Nat. Mater.*, 2006, **5**, 605; (*b*) J. Zaumseil, R. H. Friend and H. Sirringhaus, *Nat. Mater.*, 2006, **5**, 69; (*c*) J. Zaumseil and H. Sirringhaus, *Chem. Rev.*, 2007, **107**, 1296; (*d*) F. Cicoira and C. Santato, *Adv. Funct. Mater.*, 2007, **17**, 3421; (*e*) S. Z. Bisri, T. Takenobu, Y. Yomogida, H. Shimotani, T. Yamao, S. Hotta and Y. Iwasa, *Adv. Funct. Mater.*, 2009, **20**, 1661; (*f*) E. B. Namdas, B. B. Y. Hsu, J. D. Yuen, D. W. Samuel and A. J. Heeger, *Adv. Mater.*, 2011, **23**, 2353.

6 (*a*) I. D. W. Samuel and G. A. Turnbull, *Chem. Rev.*, 2007, **107**, 1272; (*b*) I. D. W. Samuel, *Nature*, 2004, **429**, 709; (*c*) K. Meerholz, B. H. Wallikewitz, M. de la Rosa, J. H. W. M. Kremer and D. Hertel, *Adv. Mater.*, 2010, **22**, 531; (*d*) X. Liu, H. Li, C. Song, Y. Liao and M. Tian, *Opt. Lett.*, 2009, **34**, 503; (*e*) R. Xia, W. Y. Lai, P. A. Levermore, W. Huang and D. D. C. Bradley, *Adv. Funct. Mater.*, 2009, **19**, 2844; (*f*) S. Kéna-Cohen and S. R. Forrest, *Nat. Photonics*, 2010, **4**, 371.

7 (*a*) D. H. Kim, D. Y. Lee, H. S. Lee, W. H. Lee, Y. H. Kim, J. I. Han and K. Cho, *Adv. Mater.*, 2007, **19**, 678; (*b*) Y. S. Zhao, A. Peng, H. Fu, Y. Ma and J. Yao, *Adv. Mater.*, 2008, **20**, 1661; (*c*) J. H. Oh, H. W. Lee, S. Mannsfeld, R. M. Stoltenberg, E. Jung, Y. W. Jin, J. M. Kim, J.-B. Yoo and Z. Bao, *Proc. Natl. Acad. Sci.*, 2009, **106**, 6065; (*d*) Y. Che, X. Yang, K. Balakrishnan, J. Zuo and L. Zang, *Chem. Mater.*, 2009, **21**, 2930; (*e*) Q. Bao, B. M. Goh, B. Yan, T. Yu, Z. Shen and K. P. Loh, *Adv. Mater.*, 2010, **22**, 3661; (*f*) Y. Zhou, T. Lei, L. Wang, J. Pei, Y. Cao and J. Wang, *Adv. Mater.*, 2010, **22**, 1484; (*g*) H. Mizuno, I. Ohnishi, H. Yanagi, F. Sasaki and Shu Hotta, *Adv. Mater.*, 2012, **24**, 2404; (*h*) H. Mizuno, U. Haku, Y. Marutani, A. Ishizumi, H. Yanagi, F. Sasaki and S. Hotta, *Adv. Mater.*, 2012, **24**, 5744.

8 (*a*) M. O'Neill and S. M. Kelly, *Adv. Mater.*, 2003, **15**, 1135; (*b*) J. W. Goodby, I. M. Saez, S. J. Cowling, V. Görtz, M. Draper, A. W. Hall, S. Sia, G. Cosquer, S. E. Lee and E. P. Raynes, *Angew. Chem., Int. Ed.*, 2008, **47**, 2754; (*c*) S. Laschat, A. Baro, N. Steinke, F. Giesselmann, C. Hägele, G. Scalia, R. Judele, E. Kapatsina, S. Sauer, A. Schreivogel and M. Tosoni, *Angew. Chem., Int. Ed.*, 2007, **46**, 4832; (*d*) H. Yu, T. Kobayashi and H. Yang, *Adv. Mater.*, 2011, **23**, 3337; (*e*) M. O'Neill and S. M. Kelly, *Adv. Mater.*, 2011, **23**, 566.

9 (*a*) S. K. Ghosh, *Self-healing Materials: Fundamentals, Design Strategies, and Applications*, Wiely-VCH, Weinheim, Germany, 2009; (*b*) S. van der Zwaag, *Self-Healing Materials*, Springer, Dordrecht, 2007.

10 (*a*) S. Qu, X. Chen, X. Shao, F. Li, H. Zhang, H. Wang, P. Zhang, Z. Yu, K. Wu, Y. Wang and M. Li, *J. Mater. Chem.*, 2008, **18**, 3954; (*b*) S. Qu and M. Li, *Tetrahedron*, 2007, **63**, 12429; (*c*) S. Qu, L. Zhao, Z. Xiu and M. Li, *Langmuir*, 2009, **25**, 1713; (*d*) S. Qu, L. Wang, X. Liu and M. Li, *Chem.–Eur. J.*, 2011, **17**, 3512; (*e*) S. Qu, Q. Lu, S. Wu, L. Wang and X. Liu, *J. Mater. Chem.*, 2012, **22**, 24605.

11 (*a*) S. Qu, Y. Li, L. Wang, Q. Lu and X. Liu, *Chem. Commun.*, 2011, **47**, 4207; (*b*) S. Qu, H. Wang, W. Zhu, J. Luo, Y. Fan, L. Song, H. Zhang and X. Liu, *J. Mater. Chem.*, 2012, **22**, 3875.

12 B. König and H. Butenschön, *Memofix Organische Chemie*, 2nd ed, Wiley VCH, Weinheim, 1999.

13 (*a*) Y. Zhao and D. G. Trublar, *Theor. Chem. Acc.*, 2008, **120**, 215; (*b*) Y. Zhao and D. G. Trublar, *Acc. Chem. Res.*, 2008, **41**, 157.

14 (*a*) F. Würthner, C. Thalacker, S. Diele and C. Tschierske, *Chem.–Eur. J.*, 2001, **7**, 2245; (*b*) F. C. Spano, *Acc. Chem. Res.*, 2010, **43**, 429; (*c*) F. Würthner, T. E. Kaiser and C. R. Saha-Möller, *Angew. Chem., Int. Ed.*, 2011, **50**, 3376.